

Prescribed-Time Distributed Generalized Nash Equilibrium Seeking

Liraz Mudrik, Isaac Kaminer, Sean Kragelund, and Abram H. Clark

Abstract—This paper proposes the first fully distributed algorithm for finding the Generalized Nash Equilibrium (GNE) of a non-cooperative game with shared coupling constraints and general cost coupling at a user-prescribed finite time T . As a foundation, a centralized gradient-based prescribed-time convergence result is established for the GNE problem, extending the optimization Lyapunov function framework to gradient dynamics, the only known realization among existing alternatives that naturally decomposes into per-agent computations. Building on this, a fully distributed architecture is designed in which each agent concurrently runs three coupled dynamics: a prescribed-time distributed state observer, a gradient-based optimization law, and a dual consensus mechanism that enforces the shared-multiplier requirement of the variational GNE, thus guaranteeing convergence to the same solution as the centralized case. The simultaneous operation of these layers creates bidirectional perturbations between consensus and optimization, which are resolved through gain synchronization that matches the temporal singularities of the optimization and consensus layers, ensuring all error components vanish exactly at T . The Fischer-Burmeister reformulation renders the algorithm projection-free and guarantees constraint satisfaction at the deadline. Numerical simulations on a Nash-Cournot game and a time-critical sensor coverage problem validate the approach.

Index Terms—Multi-agent systems, Lyapunov methods, control-centric optimization methods, game theory, prescribed-time control, gradient methods

I. INTRODUCTION

OPTIMIZATION and equilibrium seeking in multi-agent networks have become fundamental problems in modern control theory, driven by the need to coordinate large-scale decentralized systems. The generalized Nash equilibrium problem (GNEP), where agents optimize individual objective functions subject to shared coupling constraints, is particularly relevant for resource allocation tasks where one agent's decision restricts the feasible set of others [1], [2]. Applications of GNEPs span a wide range of critical infrastructure, including demand-side management in smart grids [3], coordinated

trajectory planning for robotic swarms [4], and competitive power control in communication networks [5].

Given the scale, privacy, and hardware requirements of these systems, centralized solutions are often impractical. Consequently, the research focus has shifted to distributed algorithms where agents communicate only with local neighbors. Extensive work has been done on distributed GNE seeking using primal-dual dynamics [6], [7], operator splitting methods [8], [9], penalty-based approaches [10], [11], and consensus-based schemes [12]; see [13], [14] for comprehensive surveys. These methods handle general cost coupling and shared constraints, but rely on asymptotic convergence.

While asymptotic stability is sufficient for many scenarios, it is often inadequate for safety-critical cyber-physical systems operating under hard real-time constraints. In applications such as missile guidance [15], competitive resource allocation in multi-cluster networks [16], or collision avoidance [17], agents must agree on a valid solution by a strict deadline to prevent system failure. Standard distributed algorithms, which typically exhibit linear or exponential convergence rates [18], cannot provide such guarantees, as their settling times depend heavily on initial conditions and network connectivity.

To address the need for faster convergence, recent research has explored finite-time [19] and fixed-time [20] stability. Finite-time methods [21] guarantee convergence in finite time, but the settling time remains dependent on initial states. Fixed-time methods [22] provide a uniform upper bound independent of initial conditions, and have been applied to Nash equilibrium seeking in [23]. However, these bounds are often conservative and difficult to tune for a precise deadline, limiting their utility in time-critical coordination.

The most recent advancement is *prescribed-time* control [24], [25], which employs time-varying gains to force exact convergence at a user-defined time, independent of initial conditions. This paradigm has been successfully applied to consensus problems [26], centralized optimization [27], and distributed Nash equilibrium seeking for standard (uncoupled) games [28], [29]. However, none of these methods simultaneously addresses shared coupling constraints and user-prescribed convergence deadlines for GNEPs.

This paper proposes a fully distributed algorithm for general GNE seeking that achieves exact convergence at a prescribed time. Recent work [30] addresses predefined-time convergence, where the upper bound of the convergence time can be set by the user, for aggregative games, a restricted GNEP subclass where costs depend on local decisions and an aggregative

This work was supported in part by the Office of Naval Research Science of Autonomy Program under Grant No. N0001425GI01545 and Consortium for Robotics Unmanned Systems Education and Research at the Naval Postgraduate School.

L. Mudrik, I. Kaminer, and S. Kragelund are with the Department of Mechanical and Aerospace Engineering, Naval Postgraduate School, Monterey, CA, 93943, USA (e-mail: liraz.mudrik.ctr@nps.edu; kaminer@nps.edu; spkragel@nps.edu).

A. H. Clark is with the Department of Physics, Naval Postgraduate School, Monterey, CA, 93943, USA (e-mail: abe.clark@nps.edu).

gate of all decisions rather than the full decision profile. Our algorithm converges in prescribed time, a stronger guarantee ensuring exact convergence at the deadline rather than merely an upper bound [25], and handles the standard GNEP class studied in the distributed GNE literature (e.g., in [6], [7], [11]), with arbitrary functional coupling in costs and shared constraints, encompassing applications such as pairwise collision avoidance and bilateral contracts where full decision vector estimation is unavoidable. A critical enabling component of the distributed architecture is the state estimation layer. Existing prescribed-time consensus results, such as [26], address only static leaders; the self-anchored observer of [31] tracks moving leaders but achieves only asymptotic convergence. The distributed GNE setting requires exact prescribed-time tracking of leaders whose states are themselves driven by coupled optimization dynamics—a combination that neither reference establishes and that constitutes a separate contribution of this work. The proposed architecture is simultaneous: each agent concurrently runs a prescribed-time distributed state observer to estimate the full network state, a gradient-based optimization law, and a dual consensus mechanism that enforces the variational GNE (v-GNE), yielding the same solution as the centralized case [8].

The main contributions of this work are fourfold. First, we extend the optimization Lyapunov function (OLF) framework for GNEPs of [27] to gradient dynamics, an OLF realization that naturally decomposes into per-agent computations, and establish a centralized prescribed-time convergence result for GNE seeking. Second, we propose a prescribed-time distributed state observer for networks with optimization-driven moving leaders. Inspired by the prescribed-time scaling mechanism of [26] and the self-anchored observer architecture of [31], this observer achieves exact prescribed-time convergence in the moving-leader setting that neither reference addresses. Third, we propose the first fully distributed prescribed-time GNE seeking algorithm, featuring three simultaneously coupled layers: primal consensus, optimization, and dual updates with consensus, the latter of which is absent from all prior prescribed-time NE works [28], [29] and is essential for v-GNEs. Fourth, we provide convergence guarantees via a composite time-varying Lyapunov function built around a network potential that unifies optimization residuals, consensus errors, and dual disagreements. Table I summarizes the key distinctions between the proposed distributed algorithm and existing distributed Nash equilibrium-seeking methods.

The remainder of this paper is organized as follows. Section II formulates the GNE problem and states the standing assumptions. Section III develops the centralized gradient-based GNE seeking result. Section IV details the distributed control architecture. Section V provides the theoretical convergence analysis. Section VI presents numerical results, followed by concluding remarks.

II. PROBLEM FORMULATION

We consider a network of N agents interacting over a communication graph $\mathcal{G} = (\mathcal{V}, \mathcal{E})$, where $\mathcal{V} = \{1, \dots, N\}$ is the set of agents and $\mathcal{E} \subseteq \mathcal{V} \times \mathcal{V}$ is the set of edges representing

communication links. The graph is assumed to be undirected and connected. The adjacency matrix $\mathcal{A} = [a_{ij}] \in \mathbb{R}^{N \times N}$ is defined such that $a_{ij} > 0$ if $(j, i) \in \mathcal{E}$ and $a_{ij} = 0$ otherwise. The Laplacian matrix $\mathcal{L} \in \mathbb{R}^{N \times N}$ is defined as $\mathcal{L} = \mathcal{D} - \mathcal{A}$, where \mathcal{D} is the degree matrix. For a connected graph, \mathcal{L} is positive semi-definite, with a single zero eigenvalue corresponding to the eigenvector of ones, $\mathbf{1}_N$; we denote by $\lambda_2(\mathcal{L}) > 0$ the smallest positive eigenvalue (algebraic connectivity). We denote the Kronecker product by \otimes and the Euclidean norm by $\|\cdot\|$. For a stack of vectors $\mathbf{x}_1, \dots, \mathbf{x}_N$, we denote the aggregate vector as $\mathbf{x} = \text{col}(\mathbf{x}_1, \dots, \mathbf{x}_N)$.

The agents engage in a non-cooperative game where each agent $i \in \mathcal{V}$ controls a local decision variable $\mathbf{x}_i \in \mathbb{R}^{n_i}$. The global decision vector is denoted by $\mathbf{x} = \text{col}(\mathbf{x}_1, \dots, \mathbf{x}_N) \in \mathbb{R}^n$, where $n = \sum_{i=1}^N n_i$. Each agent aims to minimize its local objective function $J_i(\mathbf{x}_i, \mathbf{x}_{-i})$, which depends on its own decision \mathbf{x}_i and the decisions of other agents \mathbf{x}_{-i} . The optimization is subject to shared coupling constraints. Specifically, the problem for agent i is formulated as:

$$\min_{\mathbf{x}_i} J_i(\mathbf{x}_i, \mathbf{x}_{-i}) \quad (1a)$$

$$\text{s.t. } \mathbf{A}\mathbf{x} = \mathbf{b}, \quad (1b)$$

$$\mathbf{g}(\mathbf{x}) \leq \mathbf{0}, \quad (1c)$$

where $\mathbf{A} \in \mathbb{R}^{m \times n}$ and $\mathbf{b} \in \mathbb{R}^m$ define shared affine equality constraints, and $\mathbf{g} : \mathbb{R}^n \rightarrow \mathbb{R}^p$ represents shared inequality constraints.

A strategy profile $\mathbf{x}^* = \text{col}(\mathbf{x}_1^*, \dots, \mathbf{x}_N^*)$ is a GNE if no agent can unilaterally reduce its cost while remaining feasible, given the decisions of all other agents. Formally, for every $i \in \mathcal{V}$,

$$J_i(\mathbf{x}_i^*, \mathbf{x}_{-i}^*) \leq J_i(\mathbf{x}_i, \mathbf{x}_{-i}^*), \quad \forall \mathbf{x}_i \in \mathcal{X}_i(\mathbf{x}_{-i}^*), \quad (2)$$

where the feasible set available to agent i , given the other agents' decisions, is

$$\mathcal{X}_i(\mathbf{x}_{-i}) = \left\{ \mathbf{x}_i \in \mathbb{R}^{n_i} : \mathbf{A}\mathbf{x} = \mathbf{b}, \mathbf{g}(\mathbf{x}) \leq \mathbf{0} \right\} \Big|_{\mathbf{x}=(\mathbf{x}_i, \mathbf{x}_{-i})}, \quad (3)$$

and $(\mathbf{x}_i, \mathbf{x}_{-i})$ denotes the global decision vector with the i -th block replaced by \mathbf{x}_i . The coupling in the constraints, where agent i 's feasible set $\mathcal{X}_i(\mathbf{x}_{-i})$ depends on the decisions of others, is what distinguishes the GNEP from a standard Nash equilibrium problem.

To guarantee the existence, uniqueness, and solvability of the GNEP, we employ the following standard assumptions regarding the network topology and the optimization structure.

Assumption 2.1 (Graph Connectivity): The communication graph \mathcal{G} is undirected and connected. This ensures that information can propagate between any pair of agents, allowing for the distributed estimation of global variables.

Assumption 2.2 (Strong Monotonicity): Define the pseudo-gradient mapping

$$\mathbf{F}(\mathbf{x}) := \text{col}(\nabla_{\mathbf{x}_1} J_1, \dots, \nabla_{\mathbf{x}_N} J_N). \quad (4)$$

$\mathbf{F}(\mathbf{x})$ is strongly monotone with respect to \mathbf{x} , that is, there exists a constant $m_F > 0$ such that for all $\mathbf{x}, \mathbf{y} \in \mathbb{R}^n$:

$$(\mathbf{F}(\mathbf{x}) - \mathbf{F}(\mathbf{y}))^\top (\mathbf{x} - \mathbf{y}) \geq m_F \|\mathbf{x} - \mathbf{y}\|^2. \quad (5)$$

TABLE I
COMPARISON WITH EXISTING DISTRIBUTED NE/GNE SEEKING METHODS.

Feature	[12]	[6]–[8], [10], [11]	[16]	[23]	[28]	[29]	[30]	Ours
Game class	NE	GNE	NE	NE	NE	NE	GNE	GNE
Shared constraints	×	✓	×	×	×	×	✓	✓
General cost coupling	✓	✓	✓	✓	✓	✓	×	✓
Convergence rate	Asymptotic	Asymptotic	Exponential	Fixed-time	Prescribed	Prescribed	Predefined	Prescribed
Fully distributed	✓	✓	×	✓	✓	✓	✓	✓
Full decision info.	✓	✓	✓	✓	✓	✓	×	✓
Graph type	Undirected	Undirected	Undirected	Undirected	Undirected	Directed	Undirected	Undirected

The strong monotonicity assumption ensures the existence and uniqueness of the v-GNE [1], and implies global convergence of gradient-based methods.

Assumption 2.3 (Smoothness and Constraint Convexity):

The cost functions J_i and constraint functions \mathbf{g} are twice continuously differentiable, the equality constraint matrix A has full row rank, and each component g_j of \mathbf{g} is convex.

Assumption 2.4 (Generalized Slater's Condition): There exists a strictly feasible point $\bar{\mathbf{x}} \in \mathbb{R}^n$ satisfying:

$$A\bar{\mathbf{x}} = \mathbf{b}, \quad \mathbf{g}(\bar{\mathbf{x}}) < \mathbf{0}, \quad (6)$$

where the inequality holds component-wise. This ensures that the Karush-Kuhn-Tucker (KKT) conditions are necessary and sufficient for the v-GNE, and that strong duality holds [1].

Assumption 2.5 (Restricted Lagrangian Strong Convexity):

Define the generalized Lagrangian Hessian

$$H_L(\mathbf{x}, \boldsymbol{\lambda}) \triangleq \nabla_{\mathbf{x}} \mathbf{F}(\mathbf{x}) + \sum_{j=1}^p \lambda_j \nabla^2 g_j(\mathbf{x}). \quad (7)$$

There exists a constant $m_L > 0$ such that

$$v^\top H_L(\mathbf{x}, \boldsymbol{\lambda}) v \geq m_L \|v\|^2, \quad \forall v \in \ker(A), \quad \forall \mathbf{z} \in \Omega_c, \quad (8)$$

where Ω_c is the sublevel set defined in Proposition 3.1.

Remark 2.6 (Special constraint structures): When the inequality constraints are affine, $H_L = \nabla_{\mathbf{x}} \mathbf{F} \succeq m_F I$ by Assumption 2.2, so Assumption 2.5 holds with $m_L = m_F$ for all $c > 0$. When there are no equality constraints ($m = 0$), the variable $\boldsymbol{\mu}$, the \mathbf{S}_2 block, and the $\boldsymbol{\mu}$ -consensus layer are absent; Assumption 2.5 then requires $v^\top H_L v \geq m_L \|v\|^2$ for all $v \in \mathbb{R}^n$ rather than only $v \in \ker(A)$, which again reduces to strong monotonicity in the affine case. Both simplifications apply to the examples of Section VI.

Under these assumptions, we focus on finding a v-GNE, a refinement of the GNE concept in which all agents share identical dual multipliers for the coupling constraints. A point \mathbf{x}^* is a v-GNE if it solves the variational inequality $\text{VI}(\mathbf{F}, \mathcal{X})$, where $\mathcal{X} = \{\mathbf{x} : A\mathbf{x} = \mathbf{b}, \mathbf{g}(\mathbf{x}) \leq \mathbf{0}\}$ is the shared feasible set and \mathbf{F} is the pseudo-gradient mapping. Under Slater's condition, the v-GNE is characterized by the KKT conditions with shared multipliers [1]. Let $\boldsymbol{\lambda} \in \mathbb{R}^p$ and $\boldsymbol{\mu} \in \mathbb{R}^m$ denote the dual multipliers associated with the inequality and equality constraints, respectively. A point $\mathbf{z}^* = \text{col}(\mathbf{x}^*, \boldsymbol{\lambda}^*, \boldsymbol{\mu}^*)$ is a primal-dual solution if it satisfies:

$$\mathbf{F}(\mathbf{x}^*) + \nabla \mathbf{g}(\mathbf{x}^*)^\top \boldsymbol{\lambda}^* + A^\top \boldsymbol{\mu}^* = \mathbf{0}, \quad (9a)$$

$$A\mathbf{x}^* - \mathbf{b} = \mathbf{0}, \quad (9b)$$

$$\mathbf{g}(\mathbf{x}^*) \leq \mathbf{0}, \quad \boldsymbol{\lambda}^* \geq \mathbf{0}, \quad \langle \boldsymbol{\lambda}^*, \mathbf{g}(\mathbf{x}^*) \rangle = 0. \quad (9c)$$

This distinguishes the v-GNE from the broader class of GNEs, in which each agent may hold different dual multipliers that satisfy only local optimality conditions.

III. CENTRALIZED GRADIENT-BASED GNE SEEKING

This section develops a centralized gradient-based prescribed-time algorithm for the GNEP, where a single entity has access to the full primal-dual state. The result serves two purposes: it provides the theoretical template that the distributed architecture of Sec. IV realizes, and it extends the OLF framework of [27] from the Hessian-gradient dynamics to the gradient dynamics required for distributed implementation.

A. Stationarity Mapping and the Optimization Lyapunov Function

We adopt the control-centric optimization framework introduced in [27]. Rather than proposing update dynamics and analyzing their convergence post hoc, this approach treats the augmented primal-dual state as a plant with single integrator dynamics

$$\dot{\mathbf{z}} = \mathbf{u}, \quad (10)$$

where \mathbf{u} is a feedback law to be designed. We define the global augmented state $\mathbf{z} = \text{col}(\mathbf{x}, \boldsymbol{\lambda}, \boldsymbol{\mu}) \in \mathbb{R}^{n+p+m}$. The first-order optimality (KKT) conditions from (9) are encoded into a single stationarity vector $\mathbf{S}(\mathbf{z}) \in \mathbb{R}^{n+p+m}$, defined as:

$$\mathbf{S}(\mathbf{z}) = \begin{bmatrix} \mathbf{S}_1(\mathbf{z}) \\ \mathbf{S}_2(\mathbf{z}) \\ \mathbf{S}_3(\mathbf{z}) \end{bmatrix} = \begin{bmatrix} \mathbf{F}(\mathbf{x}) + \nabla \mathbf{g}(\mathbf{x})^\top \boldsymbol{\lambda} + A^\top \boldsymbol{\mu} \\ A\mathbf{x} - \mathbf{b} \\ \Phi_\epsilon(\boldsymbol{\lambda}, -\mathbf{g}(\mathbf{x})) \end{bmatrix}, \quad (11)$$

where \mathbf{S}_1 captures stationarity, \mathbf{S}_2 captures primal feasibility of the equality constraints, and \mathbf{S}_3 captures the conditions related to the inequality constraints. The term $\Phi_\epsilon(\boldsymbol{\lambda}, -\mathbf{g}(\mathbf{x}))$ represents the smoothed Fischer-Burmeister function applied element-wise [32], [33]:

$$\Phi_\epsilon(a, b) = \sqrt{a^2 + b^2 + \epsilon^2} - (a + b), \quad (12)$$

with smoothing parameter $\epsilon > 0$. The smoothed FB function satisfies $\Phi_\epsilon(a, b) = 0$ if and only if $a \geq 0$, $b \geq 0$, and $ab = \epsilon^2/2$. Consequently, $\mathbf{S}(\mathbf{z}) = \mathbf{0}$ encodes the ϵ -approximate KKT conditions: stationarity (first block), primal feasibility (second block), and a relaxed complementarity condition $\lambda_j g_j(\mathbf{x}) = -\epsilon^2/2$ that recovers exact complementarity as $\epsilon \rightarrow 0$.

We define the OLF for the plant (10) as the squared norm of the stationarity vector:

$$V(\mathbf{z}) = \frac{1}{2} \|\mathbf{S}(\mathbf{z})\|^2. \quad (13)$$

The optimization design objective is to choose \mathbf{u} such that the OLF decays to zero according to a user-prescribed profile. Because constraint satisfaction is enforced by driving \mathbf{S} to zero rather than by projecting onto the feasible set, the resulting dynamics are entirely projection-free. During the transient phase $t < T$, constraint violation is bounded on $\Omega_{V(0)}$; at $t = T$, $\mathbf{S}(\mathbf{z}) = 0$ enforces $A\mathbf{x} = \mathbf{b}$ exactly and the inequality constraints to within $O(\epsilon)$.

B. Sublevel Set Compactness

A key requirement for the convergence analysis is that trajectories remain bounded. In standard Lyapunov-based stability analyses, this is ensured by assuming radial unboundedness of the Lyapunov function, i.e., $V(\mathbf{z}) \rightarrow \infty$ whenever $\|\mathbf{z}\| \rightarrow \infty$, which guarantees that sublevel sets are compact. However, the OLF $V = \frac{1}{2} \|\mathbf{S}\|^2$ is *not* radially unbounded for GNEPs with nonlinear inequality constraints.

The obstruction is a dual escape direction: if $\lambda_j \rightarrow +\infty$ while \mathbf{x} approaches a minimizer of g_j , then $\lambda_j \nabla g_j(\mathbf{x})$ remains bounded in \mathbf{S}_1 and $\Phi_\epsilon(\lambda_j, -g_j(\mathbf{x})) \rightarrow \min_{\mathbf{x}} g_j(\mathbf{x})$ (see Subcase C2, Appendix I), so $\|\mathbf{z}\| \rightarrow \infty$ while $V(\mathbf{z})$ stays finite. The following result shows V cannot remain below c^* along any escape direction, restoring compactness.

Proposition 3.1 (Sublevel Set Compactness): Under Assumptions 2.2–2.4, define the compactness threshold

$$c^* \triangleq \frac{1}{2} \min_{j=1, \dots, p} \left(\min_{\mathbf{x} \in \mathbb{R}^n} g_j(\mathbf{x}) \right)^2. \quad (14)$$

Then, $c^* > 0$ and for all $0 < c < c^*$, the sublevel set

$$\Omega_c = \{\mathbf{z} \in \mathbb{R}^{n+p+m} : V(\mathbf{z}) \leq c\}$$

is compact. Moreover, if $\mathbf{g}(\mathbf{x}) = \mathbf{C}\mathbf{x} - \mathbf{d}$ where $\mathbf{C} \in \mathbb{R}^{p \times n}$ has full row rank, then $c^* = +\infty$ and Ω_c is compact for all $c > 0$.

The proof is deferred to Appendix I. The threshold c^* depends only on the inequality constraint functions and is independent of the cost functions, communication graph, or algorithm gains. It quantifies the margin provided by Slater's condition: more strictly feasible constraints yield a larger c^* . For affine constraints, the constraint gradient never vanishes, so no dual escape direction exists and $c^* = +\infty$.

Lemma 3.2 (Non-Singularity of $\nabla \mathbf{S}$): Under Assumptions 2.2, 2.3, and 2.5, for any $\epsilon > 0$, the Jacobian $\nabla \mathbf{S}(\mathbf{z})$ is non-singular for every $\mathbf{z} \in \Omega_c$. Consequently, the uniform lower bound

$$\underline{\sigma} \triangleq \min_{\mathbf{z} \in \Omega_c} \sigma_{\min}(\nabla \mathbf{S}(\mathbf{z})) > 0 \quad (15)$$

holds, where compactness of Ω_c is guaranteed by Proposition 3.1.

Proof: The Jacobian of $\mathbf{S}(\mathbf{z})$ with respect to $\mathbf{z} = \text{col}(\mathbf{x}, \boldsymbol{\lambda}, \boldsymbol{\mu})$ has the block structure

$$\nabla \mathbf{S}(\mathbf{z}) = \begin{pmatrix} H_L(\mathbf{x}, \boldsymbol{\lambda}) & \nabla \mathbf{g}(\mathbf{x})^\top & A^\top \\ A & 0 & 0 \\ -D_b \nabla \mathbf{g}(\mathbf{x}) & D_\mu & 0 \end{pmatrix}, \quad (16)$$

where $D_b = \text{diag}(\partial_b \Phi_\epsilon(\lambda_j, -g_j(\mathbf{x})))$ is diagonal with entries $\partial_b \Phi_\epsilon \in (-2, 0)$, arising from differentiating $\Phi_\epsilon(\lambda_j, -g_j(\mathbf{x}))$ with respect to \mathbf{x} (yielding the (3,1) block $-D_b \nabla \mathbf{g}(\mathbf{x})$), and $D_\mu = \text{diag}(\partial_a \Phi_\epsilon(\lambda_j, -g_j(\mathbf{x})))$ is diagonal with entries $\partial_a \Phi_\epsilon \in (-2, 0)$, arising from differentiating with respect to λ_j (yielding the (3,2) block D_μ). For $\epsilon > 0$, both partial derivatives satisfy $\partial_a \Phi_\epsilon, \partial_b \Phi_\epsilon \in (-2, 0)$ strictly at every point, so $D_\mu \prec 0$ and D_μ is invertible.

Suppose $\nabla \mathbf{S}(\mathbf{z})v = 0$ for some $v = \text{col}(v_1, v_2, v_3)$. From block row 2, $Av_1 = 0$, i.e., $v_1 \in \ker(A)$. From block row 3, since D_μ is invertible,

$$v_2 = D_\mu^{-1} D_b \nabla \mathbf{g}(\mathbf{x}) v_1. \quad (17)$$

Substituting into block row 1 and taking the inner product with v_1 , while using $Av_1 = 0$ to eliminate v_3 :

$$v_1^\top \underbrace{[H_L + \nabla \mathbf{g}^\top D_\mu^{-1} D_b \nabla \mathbf{g}]}_{\hat{H}} v_1 = 0. \quad (18)$$

Since $D_\mu^{-1} \prec 0$ and $D_b \prec 0$, their product satisfies $D_\mu^{-1} D_b \succ 0$, so the second term in \hat{H} is positive semi-definite. Therefore $v_1^\top \hat{H} v_1 \geq v_1^\top H_L v_1$, and Assumption 2.5 yields $v_1^\top \hat{H} v_1 \geq m_L \|v_1\|^2 > 0$ for $v_1 \neq 0$. Hence $v_1 = 0$. Substituting back into the block-row-3 equation gives $v_2 = D_\mu^{-1} D_b \nabla \mathbf{g}(\mathbf{x}) v_1 = 0$. Block row 1 then reduces to $A^\top v_3 = 0$; since A has full row rank (Assumption 2.3), $v_3 = 0$. Thus $\nabla \mathbf{S}(\mathbf{z})$ is non-singular at every $\mathbf{z} \in \Omega_c$.

The function $\mathbf{z} \mapsto \sigma_{\min}(\nabla \mathbf{S}(\mathbf{z}))$ is continuous (as \mathbf{S} is twice continuously differentiable by Assumption 2.3) and strictly positive on Ω_c . Since Ω_c is compact (Proposition 3.1), the infimum is attained and $\underline{\sigma} > 0$. ■

C. Centralized Prescribed-Time Convergence

In the centralized setting of [27], three feedback realizations are developed for the plant (10): the Hessian-gradient dynamics (HGD), Newton dynamics (ND), and gradient dynamics (GD). The HGD normalize the gradient via

$$u = -\sigma(V, t) \nabla V / \|\nabla V\|^2, \quad (19)$$

enforcing $\dot{V} = -\sigma(V, t)$ with equality, and the ND require inverting the full Jacobian $\nabla \mathbf{S}(\mathbf{z})^{-1}$. Both yield global convergence results but require centralized information: the HGD depends on the global gradient norm $\|\nabla V\|^2$, which couples all agents' computations through a single scalar, and the ND requires the full-state Jacobian inverse, an $(n + p + m)$ -dimensional matrix. Neither admits an easy decomposition into per-agent computations.

The gradient dynamics, by contrast, employ the unnormalized feedback

$$\dot{\mathbf{z}} = -\sigma_{\text{opt}}(t) \nabla V(\mathbf{z}), \quad (20)$$

with

$$\sigma_{opt}(t) = \frac{\mu_c}{T-t}, \quad (21)$$

and $\mu_c > 0$. This structure can be decomposed, as the i -th block of this feedback,

$$\dot{\mathbf{z}}_i = -\sigma_{opt}(t) \nabla_{\mathbf{z}_i} V, \quad (22)$$

depends only on local partial derivatives of V that each agent can evaluate from its state estimates. This makes the gradient realization the natural choice, and among the three realizations in [27], the only viable candidate for distributed deployment. The price of this simplification is that the Lyapunov decay becomes an inequality rather than an equality, requiring a Polyak-Łojasiewicz (PL) condition [34] and sublevel set compactness.

Proposition 3.3 (Centralized Prescribed-Time GNEPs):

Under Assumptions 2.2–2.5, consider the gradient-based feedback (20) applied to the plant (10). If $V(\mathbf{z}(0)) < c^*$, then:

- (i) All trajectories remain bounded: $\mathbf{z}(t) \in \Omega_{V(0)}$ for all $t \in [0, T)$.
- (ii) The OLF satisfies

$$V(\mathbf{z}(t)) \leq V(\mathbf{z}(0)) \left(\frac{T-t}{T} \right)^\gamma, \quad \gamma = 2\sigma^2 \mu_c, \quad (23)$$

where $\sigma = \min_{\mathbf{z} \in \Omega_{V(0)}} \sigma_{\min}(\nabla \mathbf{S}(\mathbf{z})) > 0$.

- (iii) Consequently, $\lim_{t \rightarrow T^-} V(\mathbf{z}(t)) = 0$, and $\mathbf{z}(t)$ converges to the unique zero of the ϵ -smoothed stationarity at time T .

The proof is deferred to Appendix II. This Proposition differs from the HGD-based result of [27, Theorem VI.2] in two respects. First, the convergence guarantee is semi-global ($V(\mathbf{z}(0)) < c^*$) rather than global, because the PL condition requires compactness of the sublevel set. For GNEPs with affine inequality constraints, $c^* = +\infty$ by Proposition 3.1, so the result becomes global, recovering the same scope as the HGD. Second, the gradient dynamics rely on an inequality $\dot{V} \leq -\sigma(V, t)$ rather than the equality $\dot{V} = -\sigma(V, t)$ achieved by the HGD. The challenge addressed in the remainder of this paper is to realize the centralized gradient feedback (20) through a fully distributed architecture, where no single agent has access to the full state \mathbf{z} .

IV. DISTRIBUTED CONTROL ARCHITECTURE

In this section, we design a distributed feedback controller that solves the GNEP (1) in prescribed time $T > 0$. Guided by the centralized gradient-based result of Sec. III, we realize the centralized feedback (20) through a simultaneous architecture where agents optimize their local decision variables while concurrently estimating the global state required for gradient computation.

To handle the coupled constraints and the non-separable cost functions, each agent must estimate the full primal-dual state of the network. We define the local augmented state for agent i as:

$$\mathbf{z}_i(t) = \text{col}(\mathbf{x}_i(t), \boldsymbol{\lambda}_i(t), \boldsymbol{\mu}_i(t)) \in \mathbb{R}^{m_i}, \quad (24)$$

where $\mathbf{x}_i \in \mathbb{R}^{n_i}$ is agent i 's decision variable, and $\boldsymbol{\lambda}_i \in \mathbb{R}^p$, $\boldsymbol{\mu}_i \in \mathbb{R}^m$ are agent i 's local copies of the shared dual multipliers for the inequality and equality constraints, respectively. The total local dimension is $m_i = n_i + p + m$.

Additionally, each agent i maintains an estimate of the entire network's augmented state. To distinguish this cyber-layer estimate from the physical local variables, we denote the estimate vector by $\mathbf{y}_i(t)$:

$$\mathbf{y}_i(t) = \text{col}(\mathbf{y}_{i1}(t), \dots, \mathbf{y}_{iN}(t)) \in \mathbb{R}^{\bar{m}}, \quad (25)$$

where $\mathbf{y}_{ij}(t) \in \mathbb{R}^{m_j}$ represents agent i 's estimate of agent j 's local augmented state $\mathbf{z}_j(t)$. The total dimension is $\bar{m} = \sum_{j=1}^N m_j$.

A. Prescribed-Time Distributed State Observer

To ensure that all agents' estimates converge to the true values, each agent runs a prescribed-time distributed state observer on the estimated variables \mathbf{y}_{ij} . The gain structure is inspired by the prescribed-time scaling of [26], and the self-anchoring architecture by the asymptotic observer of [31]; as discussed in the introduction, their combination under optimization-driven moving leaders is a contribution of this work, with the formal guarantee provided by Theorem 5.1. For each target agent $j \in \mathcal{V}$, agent i updates its estimate \mathbf{y}_{ij} according to:

$$\dot{\mathbf{y}}_{ij}(t) = - \left(k_o + c_o \frac{\dot{\mu}_o(t)}{\mu_o(t)} \right) \sum_{k=1}^N a_{ik} (\mathbf{y}_{ij}(t) - \mathbf{y}_{kj}(t)), \quad (26)$$

for all $i \neq j$. Here, $k_o, c_o > 0$ are tuning gains and $\mu_o(t)$ is the time-scaling function

$$\mu_o(t) = \frac{1}{(T-t)^{\gamma_c}}, \quad \gamma_c \geq 2, \quad (27)$$

which grows unbounded as $t \rightarrow T$. Since $\dot{\mu}_o(t)/\mu_o(t) = \gamma_c/(T-t)$, the effective consensus gain in (26) becomes $\xi(t) = k_o + c_o \gamma_c/(T-t)$.

The consensus dynamics (26) alone implement a leaderless consensus: for each target agent j , the estimates $\{\mathbf{y}_{ij}\}_{i=1}^N$ would converge to a common value determined by the initial conditions $\{\mathbf{y}_{ij}(0)\}_{i=1}^N$, which generally differs from the true state $\mathbf{z}_j(t)$. To anchor the estimates to the correct value, agent j pins its own estimate to its current state [31]:

$$\mathbf{y}_{jj}(t) \equiv \mathbf{z}_j(t), \quad \forall j \in \mathcal{V}, \forall t \in [0, T). \quad (28)$$

Since agent j has direct access to $\mathbf{z}_j(t)$, no estimation is needed for its own state.

The pinning condition (28) induces N parallel leader-follower consensus problems: for the j -th block of the global state vector, agent j acts as the leader while all other agents track this moving signal via (26). This creates a bidirectional coupling: the optimization dynamics drive the leader's state $\mathbf{z}_j(t)$, while the consensus protocol propagates this change to all followers, with the prescribed-time gain ensuring that tracking errors vanish at T . The gain dominance condition $c_o > c_o^*$ in Theorem 5.1 is precisely what ensures the consensus layer absorbs this optimization-induced excitation.

B. Optimization Feedback Law with Dual Consensus

Each agent's local augmented state evolves as

$$\dot{\mathbf{z}}_i = \mathbf{u}_i, \quad (29)$$

where $\mathbf{u}_i = \text{col}(\mathbf{u}_i^x, \mathbf{u}_i^\lambda, \mathbf{u}_i^\mu)$ is the distributed feedback law designed so that all agents reach the v-GNE at the prescribed time T . The three components of \mathbf{u}_i are defined as follows.

Primal Feedback: Agent i updates its decision variable \mathbf{x}_i via gradient flow on the OLF:

$$\mathbf{u}_i^x(t) = -\sigma_{opt}(t) \nabla_{\mathbf{x}_i} V(\mathbf{y}_i(t)). \quad (30)$$

Crucially, the gradient is evaluated at the consensus estimate $\mathbf{y}_i(t)$ from (26), not the true network state; the prescribed-time consensus layer ensures this substitution becomes exact at T .

Dual Updates with Consensus: Agent i updates its dual variables λ_i and μ_i using both gradient descent and consensus with neighboring agents:

$$\begin{aligned} \mathbf{u}_i^\lambda(t) &= -N \sigma_{opt}(t) \nabla_{\lambda_i} V(\mathbf{y}_i(t)) \\ &\quad - \kappa(t) \sum_{k=1}^N a_{ik} (\lambda_i(t) - \lambda_k(t)), \end{aligned} \quad (31)$$

$$\begin{aligned} \mathbf{u}_i^\mu(t) &= -N \sigma_{opt}(t) \nabla_{\mu_i} V(\mathbf{y}_i(t)) \\ &\quad - \kappa(t) \sum_{k=1}^N a_{ik} (\mu_i(t) - \mu_k(t)), \end{aligned} \quad (32)$$

where $\sigma_{opt}(t)$ and $\kappa(t)$ are time-varying gains defined below in (33)–(34). The consensus terms in (31)–(32) force $\lambda_i \rightarrow \lambda_j$ and $\mu_i \rightarrow \mu_j$ for all i, j , ensuring the shared dual multiplier requirement of the v-GNE; without them, each agent's dual variables would converge to different values satisfying only local KKT conditions.

Remark 4.1 (Dual scaling factor): The factor N in the dual gradient terms compensates for the $1/N$ attenuation inherent in the distributed formulation. Since the centralized \mathbf{S} depends on a single shared (λ, μ) , identified in the distributed setting with the averages $\bar{\lambda} = \frac{1}{N} \sum_i \lambda_i$ and $\bar{\mu} = \frac{1}{N} \sum_i \mu_i$, the chain rule gives $\nabla_{\lambda_i} V = \frac{1}{N} \nabla_{\bar{\lambda}} V$. The scaling by N ensures that the aggregate dual descent rate $\frac{d\bar{\lambda}}{dt} = \frac{1}{N} \sum_i \dot{\lambda}_i$ matches the centralized gradient dynamics of Proposition 3.3.

The optimization and dual consensus gains contain two tuning parameters, μ_c and k_d , embedded in time-varying gains that grow unbounded as $t \rightarrow T$. Together with the consensus layer parameter c_o from (27), these three parameters govern the prescribed-time convergence. The remaining gains are the optimization layer gain:

$$\sigma_{opt}(t) = \frac{\mu_c}{T-t}, \quad \mu_c > 0, \quad (33)$$

and the dual consensus gain:

$$\kappa(t) = k_d \cdot \sigma_{opt}(t) = \frac{k_d \mu_c}{T-t}, \quad k_d > 0. \quad (34)$$

The gain synchronization $\kappa(t) = k_d \cdot \sigma_{opt}(t)$ ensures that the optimization and dual consensus dynamics share the same temporal singularity $(T-t)^{-1}$, differing only by the constant ratio k_d , enabling a unified dissipation analysis in Sec. V.

The consensus layer gains must grow sufficiently faster than the optimization gain to ensure that estimation errors decay faster than the optimization dynamics can excite them; the dual consensus ratio k_d must similarly be large enough to synchronize dual variables. The precise conditions are given in Thm. 5.1.

C. Error Coordinates and Closed-Loop Dynamics

The distributed controller presented above couples three dynamical subsystems. We introduce error coordinates that decompose the closed-loop behavior into consensus tracking, optimization progress, and dual synchronization.

Consensus Error. Let $\mathbf{e}_{ij}(t) = \mathbf{y}_{ij}(t) - \mathbf{z}_j(t)$ denote the error in agent i 's estimate of agent j 's state. By the pinning condition (28), $\mathbf{e}_{jj}(t) \equiv 0$. Define the stacked error vector for target j as $\mathbf{E}_j = \text{col}(\mathbf{e}_{1j}, \dots, \mathbf{e}_{Nj}) \in \mathbb{R}^{Nm_j}$.

Dual Disagreement. Let $\bar{\lambda}(t) = \frac{1}{N} \sum_{i=1}^N \lambda_i(t)$ and $\bar{\mu}(t) = \frac{1}{N} \sum_{i=1}^N \mu_i(t)$ denote the average dual variables. Define the disagreements $\delta_i^\lambda(t) = \lambda_i(t) - \bar{\lambda}(t)$ and $\delta_i^\mu(t) = \mu_i(t) - \bar{\mu}(t)$. Stack these as $\delta = \text{col}(\delta^\lambda, \delta^\mu) \in \mathbb{R}^{N(p+m)}$.

Optimization Residual. Since the centralized V depends on a single shared (λ, μ) , identified with the network averages in the distributed setting, we define $W_o(t) = V(\mathbf{x}(t), \bar{\lambda}(t), \bar{\mu}(t))$; per-agent dual deviations are captured by W_δ below.

In these coordinates, the closed-loop dynamics take the form:

$$\dot{\mathbf{E}}_j = -\xi(t)(\mathcal{L} \otimes I) \mathbf{E}_j - \tilde{\mathbf{1}}_j \otimes \mathbf{u}_j, \quad (35)$$

$$\dot{\delta} = -\kappa(t)(\mathcal{L} \otimes I) \delta + \boldsymbol{\eta}(t), \quad (36)$$

$$\dot{W}_o = \nabla_{\mathbf{x}} V^\top \mathbf{u}^x + \nabla_{\bar{\lambda}} V^\top \bar{\mathbf{u}}^\lambda + \nabla_{\bar{\mu}} V^\top \bar{\mathbf{u}}^\mu, \quad (37)$$

where $\tilde{\mathbf{1}}_j = \mathbf{1}_N - \mathbf{e}_j$, with \mathbf{e}_j the j -th standard basis vector in \mathbb{R}^N , accounts for the pinning condition ($\dot{\mathbf{e}}_{jj} \equiv 0$), $\bar{\mathbf{u}}^\lambda = \frac{1}{N} \sum_i \mathbf{u}_i^\lambda$ and $\bar{\mathbf{u}}^\mu = \frac{1}{N} \sum_i \mathbf{u}_i^\mu$ are the averaged dual controls, and $\boldsymbol{\eta}(t)$ is the gradient perturbation arising from heterogeneous gradient evaluations across agents. The three subsystems are bidirectionally coupled: the optimization dynamics perturb the consensus layer through \mathbf{u}_j in (35), while the consensus estimation errors corrupt the gradients in (37) and drive dual disagreement through $\boldsymbol{\eta}(t)$ in (36).

The composite Lyapunov function is built around a network potential \mathcal{V}_{net} that unifies the optimization residual and dual disagreement:

$$\mathcal{V}_{net}(t) = \underbrace{W_o(t)}_{\text{optimality}} + k_d \underbrace{W_\delta(t)}_{\text{dual agreement}}, \quad (38)$$

and the full composite function is

$$W(t) = W_c(t) + \mathcal{V}_{net}(t). \quad (39)$$

The gain synchronization $\kappa(t) = k_d \cdot \sigma_{opt}(t)$ (see (34)) ensures that the distributed dynamics approximately follow the gradient of \mathcal{V}_{net} . The control design objective in error coordinates is to establish the dissipation inequality

$$\dot{W}(t) \leq -\frac{\gamma}{T-t} W(t), \quad \gamma > 0, \quad (40)$$

which, upon integration, yields $W(t) \leq W(0) \left(\frac{T-t}{T}\right)^\gamma \rightarrow 0$ as $t \rightarrow T^-$. Theorem 5.1 establishes that tuning parameters (c_o, μ_c, k_d) satisfying (40) exist for any prescribed time T .

V. DISTRIBUTED CONVERGENCE ANALYSIS

In this section, we establish that the distributed optimizer from Sec. IV achieves prescribed-time convergence to the unique v-GNE. The analysis strategy is to construct a composite Lyapunov function $W(t)$ and show, via a contradiction argument, that $W(t) \leq W(0) < c^*$ throughout $[0, T)$. This confinement ensures $W_o \leq \mathcal{V}_{\text{net}} \leq W < c^*$, so the centralized state $(\mathbf{x}, \bar{\boldsymbol{\lambda}}, \bar{\boldsymbol{\mu}})$ remains in the compact sublevel set of Proposition 3.1, and all constants from Sec. III are valid throughout.

A. Main Convergence Result

Theorem 5.1 (Prescribed-Time Convergence to v-GNE):

Consider the GNEP (1) under Assumptions 2.1–2.5. Let agents implement the distributed controller (26)–(34). If $W(0) < c^*$, then there exist finite thresholds $c_o^*, k_d^* > 0$ such that for all $c_o > c_o^*$ and $k_d > k_d^*$:

- 1) Consensus: $\lim_{t \rightarrow T^-} \|\mathbf{y}_{ij}(t) - \mathbf{z}_j(t)\| = 0$ for all i, j .
- 2) Optimality: $\lim_{t \rightarrow T^-} V(\mathbf{z}_i(t)) = 0$ for all i .
- 3) Dual Agreement: $\lim_{t \rightarrow T^-} \|\boldsymbol{\lambda}_i(t) - \boldsymbol{\lambda}_j(t)\| = 0$ and $\lim_{t \rightarrow T^-} \|\boldsymbol{\mu}_i(t) - \boldsymbol{\mu}_j(t)\| = 0$ for all i, j .
- 4) Boundedness: All signals remain bounded on $[0, T)$.

Consequently, the system converges at time T to the unique zero $\mathbf{z}^* = (\mathbf{x}^*, \boldsymbol{\lambda}^*, \boldsymbol{\mu}^*)$ of the ϵ -smoothed stationarity vector \mathbf{S} .

The thresholds c_o^* and k_d^* depend on the problem constants $(\underline{\sigma}, \lambda_2(\mathcal{L}), L_V, \mu_c, \gamma_c)$ and can always be met by choosing c_o and k_d sufficiently large. The equilibrium \mathbf{z}^* is an ϵ -approximate v-GNE, with $\|\mathbf{z}^* - \mathbf{z}_{\text{exact}}^*\| = O(\epsilon)$ by the smoothing properties of the Fischer-Burmeister function [33]; this bound holds under the standard second-order sufficient conditions (SSOSC) and linear independence constraint qualification (LICQ) at $\mathbf{z}_{\text{exact}}^*$, which ensure the smoothed stationarity map is locally invertible via the implicit function theorem [33]. The approximation error can be made arbitrarily small by reducing ϵ . For GNEPs with affine inequality constraints, $c^* = +\infty$ by Proposition 3.1, so the initial condition imposes no restriction.

B. Proof of Theorem 5.1

The proof constructs the composite Lyapunov function $W(t) = W_c(t) + \mathcal{V}_{\text{net}}(t)$ from (39) and proceeds in five steps: (1) definition of the Lyapunov components, (2) PL condition for the network potential, (3) derivative of the network potential, (4) combined dissipation inequality with consensus, and (5) trajectory confinement and integration to obtain prescribed-time convergence. Steps 1–4 are carried out under the standing assumption that $W(t) \leq W(0)$; Step 5 verifies that this assumption is self-consistent for all $t \in [0, T)$.

Since $W(0) < c^*$ by hypothesis, the sublevel set $\Omega_{W(0)} = \{\mathbf{z} : V(\mathbf{z}) \leq W(0)\}$ is compact by Proposition 3.1 (note $\Omega_{W(0)} \supseteq \Omega_{V(0)}$ since $W(0) \geq V(\mathbf{z}(0))$; for affine constraints, $c^* = +\infty$ and the distinction is vacuous). On this set, Lemma 3.2 (under Assumption 2.5) yields the uniform lower bound $\sigma_{\min}(\nabla \mathbf{S}(\mathbf{z})) \geq \underline{\sigma} > 0$, and ∇V is Lipschitz with constant $L_V > 0$ by Assumption 2.3. With slight abuse of

notation, $\underline{\sigma}$ and L_V henceforth refer to constants computed over $\Omega_{W(0)}$.

Step 1: Composite Lyapunov Function: Recall the composite structure from (39): $W(t) = W_c(t) + \mathcal{V}_{\text{net}}(t)$, with the network potential $\mathcal{V}_{\text{net}} = W_o + k_d W_\delta$ from (38). Using the error coordinates from Section IV-C, the components are:

$$W_c(t) = \frac{1}{2} \sum_{j=1}^N \mathbf{E}_j^\top (\mathcal{L} \otimes I_{m_j}) \mathbf{E}_j, \quad (41)$$

$$W_o(t) = V(\mathbf{x}(t), \bar{\boldsymbol{\lambda}}(t), \bar{\boldsymbol{\mu}}(t)), \quad (42)$$

$$W_\delta(t) = \frac{1}{2} \boldsymbol{\delta}^\top (\mathcal{L} \otimes I_{p+m}) \boldsymbol{\delta}. \quad (43)$$

The consensus energy W_c quantifies the estimation disagreement among agents. The network potential \mathcal{V}_{net} unifies the optimality gap W_o and the dual disagreement W_δ into a single scalar function whose gradient the distributed dynamics approximately follow under gain synchronization.

Since \mathcal{G} is connected, \mathcal{L} has a simple zero eigenvalue with eigenvector $\mathbf{1}_N$, and all other eigenvalues are positive. The dual disagreement $\boldsymbol{\delta}$ is orthogonal to $\mathbf{1}_N \otimes I$ by construction (since $\sum_i \boldsymbol{\delta}_i = 0$), yielding the standard coercive bound:

$$W_\delta \geq \frac{\lambda_2(\mathcal{L})}{2} \|\boldsymbol{\delta}\|^2. \quad (44)$$

For W_c , the pinning condition $\mathbf{e}_{jj} = 0$ does not place \mathbf{E}_j orthogonal to $\mathbf{1}_N \otimes I_{m_j}$, so the standard Laplacian eigenvalue bound requires a correction. Decomposing \mathbf{E}_j into its mean $\bar{\mathbf{e}}_j = \frac{1}{N} \sum_i \mathbf{e}_{ij}$ and zero-mean component $\bar{\mathbf{E}}_j$, and noting that pinning gives $\|\bar{\mathbf{e}}_j\|^2 \leq \|\bar{\mathbf{E}}_j\|^2$, yields:

$$W_c \geq \frac{\lambda_2(\mathcal{L})}{2(1+N)} \sum_j \|\mathbf{E}_j\|^2. \quad (45)$$

Thus, $W(t) = 0$ if and only if consensus, optimality, and dual agreement are simultaneously achieved.

Step 2: PL Condition for the Network Potential: We establish a PL condition [34] for \mathcal{V}_{net} . Since V depends only on the centralized variables $(\mathbf{x}, \bar{\boldsymbol{\lambda}}, \bar{\boldsymbol{\mu}})$, the disagreement directions $\boldsymbol{\lambda}_i - \bar{\boldsymbol{\lambda}}$ lie in the null space of ∇V and must be controlled separately by the $k_d W_\delta$ term. By the chain rule, the N -scaling in (31)–(32) ensures that the effective dissipation from the optimization dynamics aggregates to $\sum_{i=1}^N [\|\nabla_{\mathbf{x}_i} V\|^2 + N \|\nabla_{\boldsymbol{\lambda}_i} V\|^2 + N \|\nabla_{\boldsymbol{\mu}_i} V\|^2] = \|\nabla_{(\mathbf{x}, \bar{\boldsymbol{\lambda}}, \bar{\boldsymbol{\mu}})} V\|^2$. By Lemma 3.2, $\|\nabla V\|^2 = \|\nabla \mathbf{S}^\top \mathbf{S}\|^2 \geq \underline{\sigma}^2 \|\mathbf{S}\|^2 = 2\underline{\sigma}^2 V$, which applied to $V = W_o$ gives $\|\nabla_{(\mathbf{x}, \bar{\boldsymbol{\lambda}}, \bar{\boldsymbol{\mu}})} V\|^2 \geq 2\underline{\sigma}^2 W_o$.

For the dual disagreement, the standard Laplacian spectral bound gives $k_d^2 \|\nabla_\delta W_\delta\|^2 \geq 2k_d^2 \lambda_2 W_\delta$. Since V is independent of $\boldsymbol{\delta}$, the squared gradient norm of \mathcal{V}_{net} decomposes additively:

$$\begin{aligned} \sum_i [\|\nabla_{\mathbf{x}_i} V\|^2 + N \|\nabla_{\boldsymbol{\lambda}_i} V\|^2 + N \|\nabla_{\boldsymbol{\mu}_i} V\|^2] + k_d^2 \|\nabla_\delta W_\delta\|^2 \\ \geq 2\alpha_{\text{net}} \mathcal{V}_{\text{net}}, \end{aligned} \quad (46)$$

where $\alpha_{\text{net}} = \min(\underline{\sigma}^2, k_d \lambda_2(\mathcal{L}))$. For k_d sufficiently large, $k_d \lambda_2 > \underline{\sigma}^2$, so that $\alpha_{\text{net}} = \underline{\sigma}^2$; this yields the threshold $k_d^* = \underline{\sigma}^2 / \lambda_2(\mathcal{L})$.

Step 3: Derivative of Network Potential: Under the gain synchronization $\kappa(t) = k_d \cdot \sigma_{opt}(t)$, we compute $\dot{V}_{net} = \dot{W}_o + k_d \dot{W}_\delta$.

Differentiating $W_o = V(\mathbf{x}, \bar{\boldsymbol{\lambda}}, \bar{\boldsymbol{\mu}})$ along the distributed dynamics, the consensus terms in (31)–(32) vanish in the dual average (since $\frac{1}{N} \sum_i (\mathcal{L} \otimes I) \boldsymbol{\lambda} = \mathbf{0}$), so the gradient descent contributions aggregate to $-\sigma_{opt}(t) \|\nabla_{(\mathbf{x}, \bar{\boldsymbol{\lambda}}, \bar{\boldsymbol{\mu}})} V\|^2$. Each agent evaluates its gradient at the estimate \mathbf{y}_i rather than the true state, introducing a Lipschitz perturbation $\boldsymbol{\eta}_i = \nabla V(\mathbf{y}_i) - \nabla V(\mathbf{z}_i)$ with $\|\boldsymbol{\eta}_i\| \leq L_V \|\mathbf{y}_i - \mathbf{z}_i\|$. Since $V = \frac{1}{2} \|\mathbf{S}\|^2$ and $\|\nabla \mathbf{S}\|$ is bounded on $\Omega_{W(0)}$, the chain rule gives $\|\nabla V\| \leq \|\nabla \mathbf{S}\| \|\mathbf{S}\| \leq M_S \sqrt{2V_{net}}$ where $M_S = \max_{\Omega_{W(0)}} \|\nabla \mathbf{S}\|$; each cross-term $\langle \nabla V, \boldsymbol{\eta}_i \rangle$ is therefore bounded by $C \sqrt{V_{net}} \cdot \sqrt{W_c}$ for a constant $C > 0$ depending on M_S, L_V, N , and $\lambda_2(\mathcal{L})$.

For the dual disagreement component, the synchronized gain yields:

$$k_d \dot{W}_\delta = -k_d^2 \sigma_{opt}(t) \boldsymbol{\delta}^\top (\mathcal{L} \otimes I)^2 \boldsymbol{\delta} + k_d \sigma_{opt}(t) \boldsymbol{\delta}^\top (\mathcal{L} \otimes I) \boldsymbol{\eta}_\delta(t), \quad (47)$$

where $\boldsymbol{\eta}_\delta(t)$ collects the heterogeneous dual gradient evaluations across agents.

Combining these, the dissipation terms from the gradient descent on W_o (including the N -scaling on the dual gradients from (31)–(32)) and the Laplacian dissipation on $k_d W_\delta$ yield:

$$\dot{V}_{net} \leq -\sigma_{opt}(t) \left[\sum_i (\|\nabla_{\mathbf{x}_i} V\|^2 + N \|\nabla_{\boldsymbol{\lambda}_i} V\|^2 + N \|\nabla_{\boldsymbol{\mu}_i} V\|^2) + k_d^2 \boldsymbol{\delta}^\top (\mathcal{L} \otimes I)^2 \boldsymbol{\delta} \right] + C_{pert} \sigma_{opt}(t) \sqrt{W_c} \sqrt{V_{net}}, \quad (48)$$

where $C_{pert} > 0$ depends on L_V, M_S, N , and $\lambda_2(\mathcal{L})$. The first bracket is precisely the squared gradient norm appearing in the PL condition (46).

Applying the PL condition (46):

$$\dot{V}_{net} \leq -2\alpha_{net} \sigma_{opt}(t) V_{net} + C_{pert} \sigma_{opt}(t) \sqrt{W_c} \sqrt{V_{net}}. \quad (49)$$

Step 4: Combined Dissipation Inequality: The consensus derivative analysis proceeds as in the standard prescribed-time observer framework [26] (under the standing requirement $\gamma_c \geq 2$ in (27)). Differentiating $W_c = \frac{1}{2} \sum_j \mathbf{E}_j^\top (\mathcal{L} \otimes I) \mathbf{E}_j$ along the error dynamics (35) and applying the squared-Laplacian bound $(\mathcal{L} \otimes I)^2 \succeq \lambda_2(\mathcal{L})(\mathcal{L} \otimes I)$ to the dissipation term yields:

$$\dot{W}_c \leq -2\xi(t) \lambda_2(\mathcal{L}) W_c + C_L \sigma_{opt}(t) \sqrt{W_c} \sqrt{V_{net}}, \quad (50)$$

where $C_L > 0$ depends on L_V, N , and the Laplacian spectrum of \mathcal{G} , and the perturbation arises from the leader dynamics $\dot{\mathbf{z}}_j$ perturbing the consensus tracking. Since $\|\dot{\mathbf{z}}_j\| = O(\sigma_{opt})$, the leader velocity also introduces a self-coupling term $O(\sigma_{opt}) W_c$, which is absorbed by $-2\xi \lambda_2 W_c$ for c_o sufficiently large via $\sigma_{opt}/\xi \leq \mu_c/(c_o \gamma_c)$.

Summing (49) and (50), and applying Young's inequality $C_{tot} \sigma_{opt} \sqrt{W_c} \sqrt{V_{net}} \leq \xi \lambda_2 W_c + \frac{C_{tot}^2 \sigma_{opt}^2}{4\xi \lambda_2} V_{net}$ with $C_{tot} = C_L + C_{pert}$ to the cross-terms $\sqrt{W_c} \sqrt{V_{net}}$:

$$\dot{W} \leq -\xi(t) \lambda_2(\mathcal{L}) W_c - \left(2\alpha_{net} - \frac{C_{tot}^2 \sigma_{opt}(t)}{4\xi(t) \lambda_2(\mathcal{L})} \right) \sigma_{opt}(t) V_{net}. \quad (51)$$

Since $\xi(t) = k_o + c_o \gamma_c / (T - t)$ and $\sigma_{opt}(t) = \mu_c / (T - t)$, the ratio $\sigma_{opt}(t)/\xi(t) = \mu_c / (k_o(T - t) + c_o \gamma_c) \leq \mu_c / (c_o \gamma_c)$ holds uniformly for all $t \in [0, T)$. This bound can be made arbitrarily small by increasing c_o . Consequently, for c_o sufficiently large, the coefficient of V_{net} in (51) is strictly positive. This establishes the existence of a finite threshold c_o^* such that for all $c_o > c_o^*$:

$$\dot{W}(t) \leq -\frac{\gamma}{T-t} W(t), \quad (52)$$

for some $\gamma > 0$.

Step 5: Trajectory Confinement and Conclusion: The dissipation inequality (52) was derived under the standing assumption that $W(t) \leq W(0)$, which ensures that all constants are evaluated on the compact set $\Omega_{W(0)}$. We now verify this assumption. Suppose for contradiction that $W(t_0) > W(0)$ for some $t_0 \in (0, T)$, and define $t^* = \inf\{t > 0 : W(t) > W(0)\}$. By continuity, $W(t) \leq W(0)$ on $[0, t^*]$ with $W(t^*) = W(0)$, so (52) holds on this interval. Integrating yields $W(t^*) \leq W(0) ((T - t^*)/T)^\gamma < W(0)$, contradicting $W(t^*) = W(0)$. Therefore $W(t) \leq W(0)$ for all $t \in [0, T)$, and (52) holds throughout.

Solving the differential inequality (52) by direct integration:

$$W(t) \leq W(0) \left(\frac{T-t}{T} \right)^\gamma. \quad (53)$$

Since $(T-t)/T \rightarrow 0$ as $t \rightarrow T^-$, we have $\lim_{t \rightarrow T^-} W(t) = 0$, which implies $W_c(T) = 0$, $W_o(T) = 0$, and $W_\delta(T) = 0$. The first gives $e_{ij}(T) = 0$ for all $i \neq j$ (consensus); the second gives $V(\mathbf{x}, \bar{\boldsymbol{\lambda}}, \bar{\boldsymbol{\mu}}) = 0$ and hence $\mathbf{S}(\mathbf{x}, \bar{\boldsymbol{\lambda}}, \bar{\boldsymbol{\mu}}) = \mathbf{0}$ (optimality); the third gives $\boldsymbol{\lambda}_i(T) = \boldsymbol{\lambda}_j(T)$ and $\boldsymbol{\mu}_i(T) = \boldsymbol{\mu}_j(T)$ for all i, j (v-GNE).

Since $W(t) \rightarrow 0$ monotonically and $\Omega_{W(0)}$ is compact, $\mathbf{S}(\mathbf{x}, \bar{\boldsymbol{\lambda}}, \bar{\boldsymbol{\mu}}) \rightarrow \mathbf{0}$ with $\bar{\boldsymbol{\lambda}} = \boldsymbol{\lambda}_i$ and $\bar{\boldsymbol{\mu}} = \boldsymbol{\mu}_i$ for all i at $t = T$. By uniqueness of the v-GNE under strong monotonicity [1], the primal solution \mathbf{x}^* is unique. The full row rank of A and the strict positivity of Φ_ϵ then uniquely determine the dual variables $(\boldsymbol{\lambda}^*, \boldsymbol{\mu}^*)$, so \mathbf{S} has a unique zero. This yields $(\mathbf{x}(T), \boldsymbol{\lambda}_i(T), \boldsymbol{\mu}_i(T)) = \mathbf{z}^*$ for all i , confirming convergence to the unique v-GNE.

Boundedness on $[0, T)$ follows from (53): since $W(t) \leq W(0)$ for all $t \in [0, T)$, the centralized state $(\mathbf{x}, \bar{\boldsymbol{\lambda}}, \bar{\boldsymbol{\mu}})$ remains in the compact sublevel set $\Omega_{W(0)}$, and the dual disagreement satisfies $\|\boldsymbol{\delta}\|^2 \leq 2W_\delta/\lambda_2 \leq 2W(0)/(k_d \lambda_2)$, so every agent's trajectory remains bounded. ■

The theoretical gains (27)–(34) diverge at $t = T$, which cannot be realized in digital implementation. In practice, one replaces $(T-t)^{-1}$ with $(T-t+\bar{\epsilon})^{-1}$ for a small $\bar{\epsilon} > 0$. Unlike the Fischer-Burmeister smoothing ϵ , which is an algorithmic design choice determining the equilibrium, $\bar{\epsilon}$ is purely a numerical artifact. The regularized analysis yields $W(T) = O(\bar{\epsilon}^\gamma)$; in our simulations, $\bar{\epsilon} = 10^{-10}$ yields final errors below 10^{-10} .

VI. NUMERICAL SIMULATIONS

We validate the proposed prescribed-time distributed GNE (PT-DGNE) algorithm in two scenarios: a standard economic benchmark (Nash-Cournot) and a time-critical cyber-physical application (Sensor Coverage).

A. Generalized Nash-Cournot Competition

We validate the algorithm on a Networked Cournot Competition with both equality and inequality constraints, using the minimal connectivity of a spanning tree topology.

1) *Setup and Parameters*: Consider $N = 20$ firms, each choosing production level $x_i \in \mathbb{R}$ to maximize profit:

$$J_i(x_i, \mathbf{x}_{-i}) = \underbrace{(\alpha_i x_i^2 + \beta_i x_i)}_{\text{Production Cost}} - x_i \underbrace{\left(P_0 - d \sum_{j=1}^N x_j \right)}_{\text{Revenue}}, \quad (54)$$

where $P_0 = 50$ is the base price, $d = 0.2$ is the price elasticity, and the cost coefficients are randomly drawn from $\alpha_i \in [1, 2]$ and $\beta_i \in [5, 10]$.

The agents are subject to shared coupling constraints:

$$\sum_{i=1}^N x_i \leq C_{max}, \quad (\text{Infrastructure Capacity}) \quad (55)$$

$$\sum_{i=1}^N r_i x_i = R_{target}, \quad (\text{Regulatory Quota}) \quad (56)$$

where $C_{max} = 40$ and $R_{target} = 40$. The weights $r_i \in [0.8, 1.2]$ represent agent-specific efficiency factors. With these parameters, both constraints are active at the equilibrium. The prescribed convergence time is $T = 10$ s with gains $\mu_c = 20$, $k_o = 50$, $c_o = 100$, and $k_d = 5$. The Fischer-Burmeister smoothing parameter is $\epsilon = 10^{-8}$, regularized with $\bar{\epsilon} = 10^{-10}$. Since the inequality constraints are affine, $c^* = +\infty$ and the initial condition of Thm. 5.1 imposes no restriction.

2) *Results*: To verify the algorithm's robustness to sparse connectivity, the agents communicate over a spanning tree topology shown in Fig. 1. Despite the low algebraic connectivity ($\lambda_2 \approx 0.096$), the prescribed-time consensus protocol ensures global information is shared effectively before the deadline.

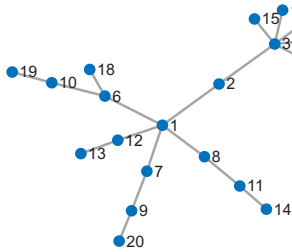


Fig. 1. Communication topology: A tree graph with $N = 20$ agents. This minimal connectivity represents a challenging scenario for distributed consensus.

Figure 2 displays the trajectories of the decision variables $x_i(t)$ for all 20 agents. Starting from identical initial conditions $x_i(0) = 5$, chosen to confirm that production differentiation arises from the optimization dynamics alone, the agents rapidly adjust their production levels. As $t \rightarrow T$, the time-varying gains enforce exact convergence to the equilibrium values $x_i^* \in [1.38, 3.07]$. The trajectories are smooth and bounded throughout the interval $[0, T]$, and the final primal error is $\|\mathbf{x}(T) - \mathbf{x}^*\| \approx 10^{-11}$.

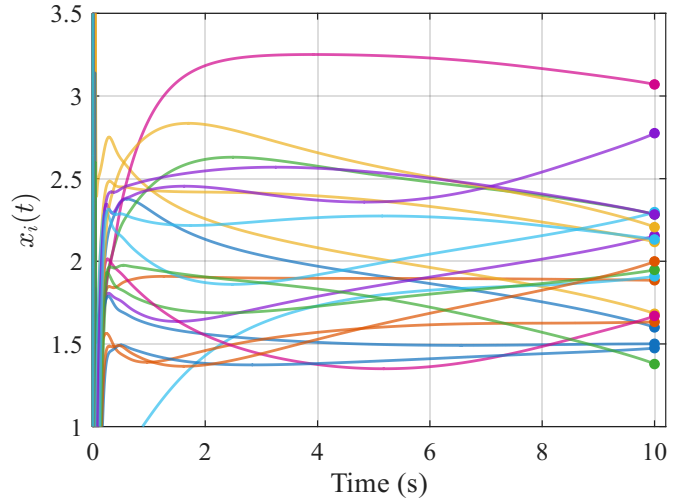


Fig. 2. Trajectories of decision variables $x_i(t)$ for $N = 20$ agents. All agents converge to their optimal production levels exactly at $T = 10$ s.

Figure 3 shows the stationarity residual $\|\mathbf{S}(\mathbf{z}(t))\|$, capturing the combined error in primal optimality, dual feasibility, and complementarity. Both the centralized benchmark and the distributed algorithm exhibit the characteristic waterfall shape of prescribed-time methods, with the residual dropping to $\approx 10^{-10}$ at the deadline. The constraint residuals at T are both below 10^{-10} , with the capacity constraint active at the solution.

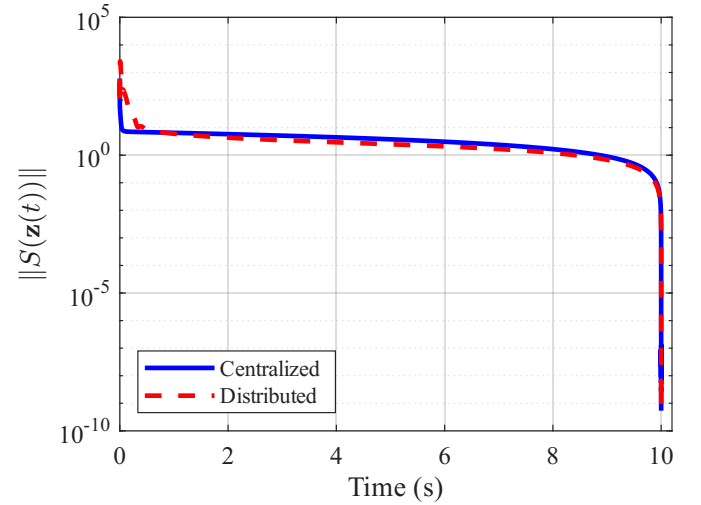


Fig. 3. Stationarity residual $\|\mathbf{S}(\mathbf{z}(t))\|$ over time. The residual decays to zero, indicating that the KKT conditions for the v-GNE are satisfied at T .

Convergence to a v-GNE additionally requires consensus on the dual variables: starting from randomized initial values $\lambda_i(0) \sim \mathcal{U}[0.5, 1.5]$ and $\mu_i(0) \sim \mathcal{U}[10, 15]$, the maximum disagreement between agents' local multiplier estimates decays to machine precision ($\approx 10^{-12}$), confirming that the dual consensus dynamics dominate the optimization-induced drift and that all agents converge to the shared shadow prices $\lambda^* \approx 32.92$ and $\mu^* \approx -4.36$.

B. Time-Critical Sensor Coverage

We now apply the algorithm to a dynamic engineering problem: optimal deployment of a mobile sensor network under shared resource constraints. Unlike the static economic example, this scenario represents a solver-in-the-loop setup where the optimization must complete exactly within the sampling interval $T_{sample} = 0.5$ s to generate valid waypoints for vehicle autopilots.

1) *Setup, Parameters, and Results:* Consider $N = 20$ mobile sensors operating in a 2D plane, \mathbb{R}^2 . The agents communicate over a spanning tree topology shown in Fig. 1. Each sensor i aims to minimize a cost function balancing target tracking and network connectivity:

$$J_i(\mathbf{x}_i, \mathbf{x}_{-i}) = \frac{1}{2} \|\mathbf{x}_i - \mathbf{b}_i\|^2 + \sum_{j \in \mathcal{N}_i} \frac{a_{ij}}{2} \|\mathbf{x}_i - \mathbf{x}_j\|^2, \quad (57)$$

where $\mathbf{x}_i \in \mathbb{R}^2$ is the position of sensor i , \mathbf{b}_i is the location of the target assigned to sensor i , and a_{ij} are the entries of the adjacency matrix.

The system is coupled by a shared power budget constraint (e.g., a total battery capacity or tethering limit). This introduces a global inequality constraint:

$$g(\mathbf{x}) = \sum_{i=1}^N \|\mathbf{x}_i\|^2 - P_{total} \leq 0. \quad (58)$$

We position the targets \mathbf{b}_i on a circle of radius $R = 15$ m, while setting P_{total} such that the maximum average deployment radius is $R_{max} = 10$ m. This configuration forces the unconstrained optimum to be infeasible, necessitating a Generalized Nash Equilibrium solution on the boundary of the feasible set.

The sensor coverage problem has a nonlinear quadratic constraint with $\min_{\mathbf{x}} g(\mathbf{x}) = -P_{total} = -2000$, yielding a compactness threshold of $c^* = \frac{1}{2} P_{total}^2 = 2 \times 10^6$ via Proposition 3.1. The initial composite Lyapunov value evaluates to $W(0) \approx 1.9 \times 10^5 \ll c^*$, confirming that the initial condition of Theorem 5.1 holds with substantial margin. As in the Cournot example, the same gains $c_o = 100$ and $k_d = 5$ are used, with Fischer-Burmeister smoothing $\epsilon = 10^{-8}$; the simulation results below confirm that these gains satisfy the gain-dominance requirement of Theorem 5.1 for this structurally different problem. Since $\nabla^2 g = 2I_n$, Assumption 2.5 reduces to requiring $\nabla_{\mathbf{x}} F(\mathbf{x}) + 2\lambda I_n \succ 0$ on $\Omega_{W(0)}$, equivalently $\lambda > -\lambda_{\min}(\nabla_{\mathbf{x}} F)/2$ throughout the trajectory; this condition is verified numerically in simulation.

We note that the pairwise coupling terms $\|\mathbf{x}_i - \mathbf{x}_j\|^2$ in the cost function prevent this problem from being formulated as an aggregative game, since each agent requires individual neighbor positions rather than a scalar aggregate. Consequently, algorithms designed for aggregative games, such as [30], are not applicable to this scenario.

The algorithm is executed with a prescribed time $T = 0.5$ s. The integration is performed using MATLAB's built-in `ode15s` function. The results are compared against a centralized prescribed-time solver implementing (20) with the same T . Wall-clock computation times on a standard desktop are 1.02 s for the centralized solver and 0.33 s per agent for the distributed algorithm. In a parallel implementation with

dedicated hardware per agent, the distributed wall-clock time is well within the $T = 0.5$ s sampling window, whereas the centralized solver exceeds it.

Figure 4 compares the norm of the stationarity residual $\|\mathbf{S}(\mathbf{z})\|$. The centralized solver (blue) and the proposed PT-DGNE algorithm (red) both drive the residual to near machine precision ($< 10^{-8}$) at $t = T$, with the distributed algorithm achieving comparable accuracy. The vertical drop on the log-scale plot confirms that the optimization process effectively terminates at the prescribed deadline, providing a mathematically exact solution for the control loop.

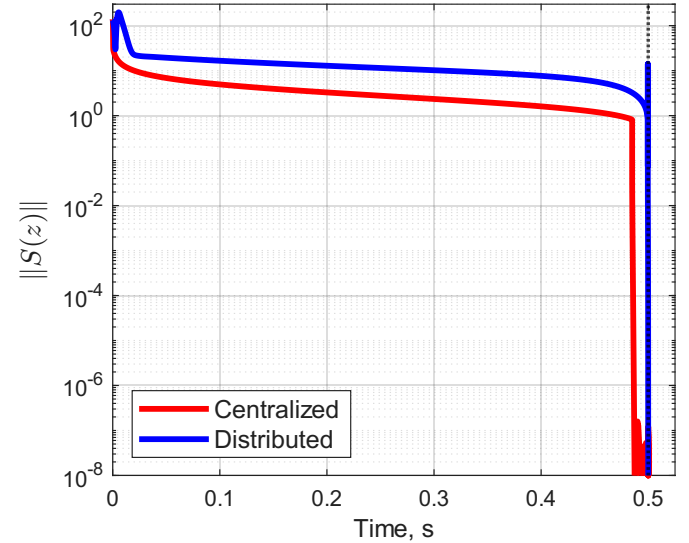


Fig. 4. Convergence of the Stationarity vector for the Sensor Network. Note the vertical drop below $\approx 10^{-8}$ at exactly $T = 0.5$ s, validating the prescribed-time property.

Figure 5 illustrates the final configuration at $t = T$. The tension is visually evident: sensors (blue) attempt to reach their targets (red) but are constrained by the power budget (dashed line). The agents automatically distribute themselves along the active constraint boundary. The shared constraint $g(\mathbf{x})$ is maintained throughout $[0, T]$ and becomes active exactly at the deadline without violation, as certified by the S_3 block of the stationarity residual converging to zero in Fig. 4.

VII. CONCLUSIONS

This paper presented a distributed control architecture for solving the GNEP under strict time constraints. A key methodological step was extending the OLF framework of [27] from the Hessian-gradient dynamics, which enforce exact Lyapunov decay but require centralized information, to the gradient dynamics that can be decomposed into per-agent computations. This extension required a Polyak-Łojasiewicz condition on compact sublevel sets, whose compactness is guaranteed by the computable threshold c^* of Proposition 3.1.

Central to the distributed architecture is the prescribed-time distributed state observer, which achieves exact prescribed-time convergence of state estimates under optimization-driven moving leaders—extending the static-leader consensus of [26] and the asymptotic self-anchored observer of [31] to the exact, time-critical setting required by the GNEP.

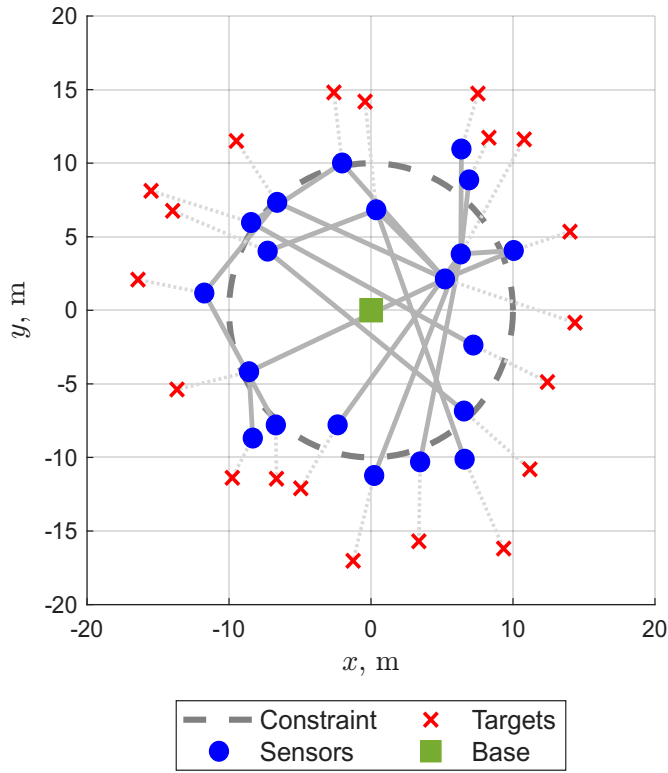


Fig. 5. Sensor Deployment at $t = T$. The sensors are distributed along the boundary of the active power constraint, balancing target tracking (dotted lines).

Building on this centralized foundation, a fully distributed feedback law was designed that achieves exact convergence to the variational GNE at a user-defined deadline T . The stability analysis employed a network potential unifying the optimization residual and dual disagreement, with gain synchronization matching the temporal singularities of the optimization and dual consensus layers to yield a unified dissipation structure. This yields tunable gain-dominance conditions on c_o and k_d that can always be satisfied for any connected topology. Numerical validation on a Nash-Cournot competition and a time-critical sensor deployment confirmed practical robustness. The sensor scenario demonstrated the algorithm's capability as a solver-in-the-loop for autonomous systems, generating optimal waypoints within a fixed sampling period. The projection-free Fischer-Burmeister formulation avoids costly feasible-set projections while guaranteeing constraint satisfaction at the deadline.

APPENDIX I PROOF OF PROPOSITION 3.1

We prove that, under Assumptions 2.2–2.4, the sublevel sets $\Omega_c = \{\mathbf{z} : V(\mathbf{z}) \leq c\}$ are compact for all $c < c^*$, and that $c^* = +\infty$ when the inequality constraints are affine.

The proof proceeds by contraposition: assuming Ω_c is unbounded for some $c < c^*$, we derive a contradiction by showing that $V(\mathbf{z}) \geq c^*$ along every escape direction. Recall the structure of the stationarity vector from (11). We show that at least one block of \mathbf{S} must be unbounded, by analyzing all possible escape directions.

Cases A–B ($\|\mathbf{x}^{(k)}\| \rightarrow \infty$ or $\|\boldsymbol{\mu}^{(k)}\| \rightarrow \infty$): Strong monotonicity gives $\|\mathbf{F}(\mathbf{x})\| \geq m_F \|\mathbf{x}\| - \|\mathbf{F}(\mathbf{0})\| \rightarrow \infty$ when $\|\mathbf{x}\| \rightarrow \infty$, and the full row rank of A gives $\|A^\top \boldsymbol{\mu}\| \geq \sigma_{\min}(A) \|\boldsymbol{\mu}\| \rightarrow \infty$ when $\|\boldsymbol{\mu}\| \rightarrow \infty$; in both cases $\|\mathbf{S}_1\| \rightarrow \infty$. Any concurrent growth of dual components either reinforces $\|\mathbf{S}_1\| \rightarrow \infty$ (via the $A^\top \boldsymbol{\mu}$ or $\nabla g^\top \boldsymbol{\lambda}$ terms) or falls into Sub-cases C1–C2 below. The remaining cases assume \mathbf{x} and $\boldsymbol{\mu}$ bounded (passing to a subsequence if necessary).

Case C ($\|\boldsymbol{\lambda}^{(k)}\| \rightarrow \infty$, \mathbf{x} bounded): This is the critical case. We consider two sub-cases.

Sub-case C1 ($\lambda_j^{(k)} \rightarrow -\infty$ for some j): Direct computation shows $\Phi_\epsilon(\lambda_j, -g_j(\mathbf{x})) = \sqrt{\lambda_j^2 + g_j(\mathbf{x})^2 + \epsilon^2} - \lambda_j + g_j(\mathbf{x}) \geq |\lambda_j| - \lambda_j + g_j(\mathbf{x}) - \sqrt{g_j(\mathbf{x})^2 + \epsilon^2} = -2\lambda_j + g_j(\mathbf{x}) - \sqrt{g_j(\mathbf{x})^2 + \epsilon^2} \rightarrow +\infty$, so $\|\mathbf{S}_3\| \rightarrow \infty$.

Sub-case C2 ($\lambda_j^{(k)} \rightarrow +\infty$ for some j , all components non-negative): By convexity of g_j , the condition $\nabla g_j(\mathbf{x}) = 0$ implies \mathbf{x} is a minimizer of g_j ; denote any such point by $\mathbf{x}_{\min,j}$. If $\|\nabla g_j(\mathbf{x}^{(k)})\| \geq \delta > 0$ for all k along the escape direction, then for affine constraints $\|\nabla g(\mathbf{x})^\top \boldsymbol{\lambda}\| \geq \sigma_{\min}(\mathbf{C}) \|\boldsymbol{\lambda}\| \rightarrow \infty$, and for nonlinear constraints the sum $\sum_j \lambda_j \nabla g_j(\mathbf{x})$ grows without bound, ensuring $\|\mathbf{S}_1\| \rightarrow \infty$ in either case.

It remains to consider the case where $\lambda_j^{(k)} \rightarrow +\infty$ and $\mathbf{x}^{(k)} \rightarrow \mathbf{x}_{\min,j}$ simultaneously, so that $\nabla g_j(\mathbf{x}^{(k)}) \rightarrow 0$. In this regime, the FB term satisfies:

$$\begin{aligned} \Phi_\epsilon(\lambda_j^{(k)}, -g_j(\mathbf{x}^{(k)})) &= \underbrace{\sqrt{(\lambda_j^{(k)})^2 + g_j(\mathbf{x}^{(k)})^2 + \epsilon^2} - \lambda_j^{(k)}}_{\rightarrow 0} \\ &+ \underbrace{g_j(\mathbf{x}^{(k)})}_{\rightarrow g_j(\mathbf{x}_{\min,j})} \rightarrow \min_{\mathbf{x}} g_j(\mathbf{x}), \end{aligned} \quad (59)$$

where the first term vanishes since $\sqrt{a^2 + c} - a \rightarrow 0$ as $a \rightarrow +\infty$ for fixed c . Thus:

$$\|\mathbf{S}_3(\mathbf{z}^{(k)})\|^2 \geq \Phi_\epsilon(\lambda_j^{(k)}, -g_j(\mathbf{x}^{(k)}))^2 \rightarrow \left(\min_{\mathbf{x}} g_j(\mathbf{x})\right)^2. \quad (60)$$

By Slater's condition (Assumption 2.4), there exists $\bar{\mathbf{x}}$ with $g_j(\bar{\mathbf{x}}) < 0$, so $\min_{\mathbf{x}} g_j(\mathbf{x}) \leq g_j(\bar{\mathbf{x}}) < 0$. Hence $V(\mathbf{z}^{(k)}) \geq \frac{1}{2}(\min_{\mathbf{x}} g_j(\mathbf{x}))^2$ along this escape direction. Taking the minimum over j :

$$\liminf_{k \rightarrow \infty} V(\mathbf{z}^{(k)}) \geq \frac{1}{2} \min_{j=1,\dots,p} \left(\min_{\mathbf{x}} g_j(\mathbf{x})\right)^2 = c^*, \quad (61)$$

which contradicts $V(\mathbf{z}^{(k)}) \leq c < c^*$. This establishes compactness for $c < c^*$.

*Positivity of c^** : By Slater's condition, $\min_{\mathbf{x}} g_j(\mathbf{x}) < 0$ for every j , so each term in the minimum is strictly positive.

Affine constraints: When $\mathbf{g}(\mathbf{x}) = \mathbf{C}\mathbf{x} - \mathbf{d}$ with \mathbf{C} having full row rank, $\nabla g_j(\mathbf{x}) = \mathbf{C}_j \neq \mathbf{0}$ for all \mathbf{x} , so the critical sub-case C2 with $\nabla g_j \rightarrow 0$ never arises. Since \mathbf{C}^\top has full column rank, $\|\mathbf{C}^\top \boldsymbol{\lambda}\| \geq \sigma_{\min}(\mathbf{C}) \|\boldsymbol{\lambda}\| \rightarrow \infty$ as $\|\boldsymbol{\lambda}\| \rightarrow \infty$, ensuring $\|\mathbf{S}_1\| \rightarrow \infty$. Hence $c^* = +\infty$. ■

APPENDIX II PROOF OF PROPOSITION 3.3

Since $V(\mathbf{z}(0)) < c^*$, the sublevel set $\Omega_{V(0)}$ is compact by Proposition 3.1, and Lemma 3.2 yields the uniform lower

bound $\underline{\sigma} > 0$ on this set. Using $\nabla V = \nabla \mathbf{S}(\mathbf{z})^\top \mathbf{S}(\mathbf{z})$ and the minimum singular value bound gives the PL condition $\|\nabla V(\mathbf{z})\|^2 \geq \underline{\sigma}^2 \|\mathbf{S}(\mathbf{z})\|^2 = 2\underline{\sigma}^2 V(\mathbf{z})$, so along (20):

$$\dot{V} = -\sigma_{opt}(t) \|\nabla V\|^2 \leq -\frac{2\underline{\sigma}^2 \mu_c}{T-t} V(\mathbf{z}). \quad (62)$$

A bootstrap contradiction argument identical to Step 5 of the proof of Theorem 5.1 (with $W_c = W_\delta = 0$ and $W = W_o = V$) establishes $V(\mathbf{z}(t)) \leq V(\mathbf{z}(0))$ for all $t \in [0, T)$, after which integrating (62) gives (23). Finite arc length ($\int_0^T \|\dot{\mathbf{z}}\| dt \leq C \int_0^T (T-t)^{\gamma/2-1} dt < \infty$ since $\gamma > 0$) confirms that $\mathbf{z}(t)$ converges to the unique zero \mathbf{z}^* of \mathbf{S} . ■

REFERENCES

- [1] F. Facchinei and C. Kanzow, "Generalized Nash Equilibrium Problems." *Annals of Operations Research*, vol. 175, no. 1, pp. 177–211, Mar. 2010.
- [2] J. B. Rosen, "Existence and Uniqueness of Equilibrium Points for Concave N-Person Games," *Econometrica*, vol. 33, no. 3, pp. 520–534, 1965.
- [3] X. Chen, C. Zhao, and N. Li, "Distributed Automatic Load Frequency Control With Optimality in Power Systems," *IEEE Transactions on Control of Network Systems*, vol. 8, no. 1, pp. 307–318, Mar. 2021.
- [4] H. Kang, C. E. Aoun, I. Kaminer, and N. Hovakimyan, "Distributed Optimal Defensive Trajectory Planning against Adversarial Swarms with Receding Horizon," in *AIAA SCITECH 2026 Forum*. American Institute of Aeronautics and Astronautics, Jan. 2026.
- [5] G. Scutari, S. Barbarossa, and D. Palomar, "Potential Games: A Framework for Vector Power Control Problems With Coupled Constraints," in *2006 IEEE International Conference on Acoustics Speech and Signal Processing Proceedings*, vol. 4, May 2006, pp. IV–IV.
- [6] L. Pavel, "Distributed GNE Seeking Under Partial-Decision Information Over Networks via a Doubly-Augmented Operator Splitting Approach," *IEEE Transactions on Automatic Control*, vol. 65, no. 4, pp. 1584–1597, Apr. 2020.
- [7] P. Yi and L. Pavel, "Distributed Generalized Nash Equilibria Computation of Monotone Games via Double-Layer Preconditioned Proximal-Point Algorithms," *IEEE Transactions on Control of Network Systems*, vol. 6, no. 1, pp. 299–311, Mar. 2019.
- [8] —, "An operator splitting approach for distributed generalized Nash equilibria computation," *Automatica*, vol. 102, pp. 111–121, Apr. 2019.
- [9] G. Belgioioso and S. Grammatico, "A distributed proximal-point algorithm for Nash equilibrium seeking in generalized potential games with linearly coupled cost functions," in *2019 18th European Control Conference (ECC)*, Jun. 2019, pp. 1–6.
- [10] A. R. Romano and L. Pavel, "An Inexact-Penalty Method for GNE Seeking in Games With Dynamic Agents," *IEEE Transactions on Control of Network Systems*, vol. 10, no. 4, pp. 2072–2084, Dec. 2023.
- [11] C. Sun and G. Hu, "Continuous-Time Penalty Methods for Nash Equilibrium Seeking of a Nonsmooth Generalized Noncooperative Game," *IEEE Transactions on Automatic Control*, vol. 66, no. 10, pp. 4895–4902, Oct. 2021.
- [12] M. Ye and G. Hu, "Distributed Nash Equilibrium Seeking by a Consensus Based Approach," *IEEE Transactions on Automatic Control*, vol. 62, no. 9, pp. 4811–4818, Sep. 2017.
- [13] G. Hu, Y. Pang, C. Sun, and Y. Hong, "Distributed Nash Equilibrium Seeking: Continuous-Time Control-Theoretic Approaches," *IEEE Control Systems Magazine*, vol. 42, no. 4, pp. 68–86, Aug. 2022.
- [14] M. Ye, Q.-L. Han, L. Ding, and S. Xu, "Distributed Nash equilibrium seeking in games with partial decision information: A survey," *Proceedings of the IEEE*, vol. 111, no. 2, pp. 140–157, Feb. 2023.
- [15] Y. Yuan, Q. Gao, H. Yuan, and X. Yue, "Cooperative Guidance Law With Impact Angle Constraint for a Multi-Leader-Multi-Follower System: A Nash Game Approach," *International Journal of Robust and Nonlinear Control*, vol. 36, no. 2, pp. 639–655, 2026.
- [16] M. Meng and X. Li, "On the linear convergence of distributed Nash equilibrium seeking for multi-cluster games under partial-decision information," *Automatica*, vol. 151, p. 110919, May 2023.
- [17] A. Shakouri and N. Assadian, "Prescribed-Time Control for Perturbed Euler-Lagrange Systems With Obstacle Avoidance," *IEEE Transactions on Automatic Control*, vol. 67, no. 7, pp. 3754–3761, Jul. 2022.
- [18] G. Qu and N. Li, "On the Exponential Stability of Primal-Dual Gradient Dynamics," *IEEE Control Systems Letters*, vol. 3, no. 1, pp. 43–48, Jan. 2019.
- [19] S. P. Bhat and D. S. Bernstein, "Finite-Time Stability of Continuous Autonomous Systems," *SIAM J. Control Optim.*, vol. 38, no. 3, pp. 751–766, Jan. 2000.
- [20] A. Polyakov, "Nonlinear Feedback Design for Fixed-Time Stabilization of Linear Control Systems," *IEEE Transactions on Automatic Control*, vol. 57, no. 8, pp. 2106–2110, Aug. 2012.
- [21] J. Cortés, "Finite-time convergent gradient flows with applications to network consensus," *Automatica*, vol. 42, no. 11, pp. 1993–2000, Nov. 2006.
- [22] K. Garg and D. Panagou, "Fixed-Time Stable Gradient Flows: Applications to Continuous-Time Optimization," *IEEE Transactions on Automatic Control*, vol. 66, no. 5, pp. 2002–2015, May 2021.
- [23] J. I. Poveda, M. Krstić, and T. Başar, "Fixed-time Nash equilibrium seeking in time-varying networks," *IEEE Transactions on Automatic Control*, vol. 68, no. 4, pp. 1954–1969, Apr. 2023.
- [24] Y. Song, Y. Wang, J. Holloway, and M. Krstic, "Time-varying feedback for regulation of normal-form nonlinear systems in prescribed finite time," *Automatica*, vol. 83, pp. 243–251, Sep. 2017.
- [25] Y. Song, H. Ye, and F. L. Lewis, "Prescribed-time control and its latest developments," *IEEE Transactions on Systems, Man, and Cybernetics: Systems*, vol. 53, no. 7, pp. 4102–4116, Jul. 2023.
- [26] Y. Wang, Y. Song, D. J. Hill, and M. Krstic, "Prescribed-Time Consensus and Containment Control of Networked Multiagent Systems," *IEEE Transactions on Cybernetics*, vol. 49, no. 4, pp. 1138–1147, Apr. 2019.
- [27] L. Mudrik, I. Kaminer, S. Kragelund, and A. H. Clark, "Optimization via a Control-Centric Framework," *arXiv preprint arXiv:2510.05455*, Oct. 2025, submitted to *IEEE Trans. Cybern.*
- [28] Y. Zhao, J. Tao, B. Xian, S. Li, and H. Duan, "Prescribed-time distributed Nash equilibrium seeking for noncooperation games," *Automatica*, vol. 151, p. 110933, May 2023.
- [29] Y. Qian and Z. Ding, "Prescribed-time fully distributed Nash equilibrium seeking strategy in networked games," *IEEE/CAA Journal of Automatica Sinica*, vol. 11, no. 1, pp. 261–263, Jan. 2024.
- [30] S. Guo, X. Zeng, S. Cheng, and M. Li, "Distributed GNE seeking for aggregative games under event-triggered communication: Predefined-time convergent algorithm design," *Neurocomputing*, vol. 657, p. 131623, Dec. 2025.
- [31] Y. Zou, B. Huang, Z. Meng, and W. Ren, "Continuous-time distributed Nash equilibrium seeking algorithms for non-cooperative constrained games," *Automatica*, vol. 127, p. 109535, May 2021.
- [32] A. Fischer, "A special newton-type optimization method," *Optimization*, vol. 24, no. 3–4, pp. 269–284, Jan. 1992.
- [33] D. Liao-McPherson, M. Huang, and I. Kolmanovsky, "A Regularized and Smoothed Fischer–Burmeister Method for Quadratic Programming With Applications to Model Predictive Control," *IEEE Transactions on Automatic Control*, vol. 64, no. 7, pp. 2937–2944, Jul. 2019.
- [34] H. Karimi, J. Nutini, and M. Schmidt, "Linear Convergence of Gradient and Proximal-Gradient Methods Under the Polyak–Łojasiewicz Condition," in *Machine Learning and Knowledge Discovery in Databases*, P. Frasconi, N. Landwehr, G. Manco, and J. Vreeken, Eds. Cham: Springer International Publishing, 2016, pp. 795–811.